BMC Cancer

RESEARCH

Open Access

Oncogenic and immunological functions of USP35 in pan-cancer and its potential as a biomarker in kidney clear cell carcinoma

Yadong Guo[1,2†], Ziyou Lin[3†], Zijing Zhou[5†], Wentao Zhang[1,2], Shiyu Mao[1,2], Zezhi Shan[4*], Pengfei Wu[1,2*] and Xudong Yao[1,2*]

Abstract

Background Ubiquitin-specific protease 35 (USP35) has gained attention as a regulator in cancer progression. However, its specific role in kidney clear cell carcinoma (KIRC) remains unclear.

Methods USP35 expression in KIRC tumor and normal tissues was evaluated using TCGA data. Correlations between USP35 expression, clinical parameters, and survival outcomes were examined. Functional enrichment analyses were performed to explore the pathways associated with USP35 expression. Immune-related analyses were conducted to assess the effect of USP35 on immune cell recruitment and neoantigen presentation. Drug sensitivity analyses were used to identify potential therapeutic agents targeting USP35.

Results USP35 was significantly overexpressed in KIRC tumor tissues compared to normal tissues, and its high expression correlated with advanced disease stages and poor survival outcomes. Gene set enrichment analysis revealed that high USP35 expression was associated with oncogenic pathways, including glycerophospholipid and linoleic acid metabolism, while low expression linked to nitrogen and purine metabolism. USP35 also modulated immune responses, affecting immune cell recruitment and neoantigen presentation, suggesting a role in immune evasion. Drug sensitivity analysis showed that high USP35 expression correlated with increased sensitivity to paclitaxel, bosutinib, and lapatinib. In vitro knockdown of USP35 significantly reduced KIRC cell proliferation, migration, and epithelial-mesenchymal transition (EMT), further supporting its role in tumor progression.

Conclusion USP35 is overexpressed in KIRC and associated with poor prognosis, likely promoting tumor progression through oncogenic pathways and immune modulation. Its correlation with drug sensitivity positions USP35 as a potential therapeutic target, warranting further investigation into its mechanistic functions and therapeutic applications.

Keywords USP35, KIRC, Prognostic biomarker, Immunotherapy

†Yadong Guo, Ziyou Lin and Zijing Zhou contributed equally to this study.

*Correspondence:
Zezhi Shan
18111230016@fudan.edu.cn
Pengfei Wu
guangmingwpf@163.com
Xudong Yao
yaoxudong1967@163.com
Full list of author information is available at the end of the article

Introduction

Cancer remains a leading cause of death worldwide, posing a significant threat to human health [1]. Kidney clear cell carcinoma (KIRC) is a highly malignant subtype of kidney cancer and one of the most prevalent cancers within the urinary system. It accounts for the majority of kidney cancer cases worldwide, with a rising incidence and mortality rate [2, 3]. Despite advancements in treatment modalities, including surgery, targeted therapies, and immunotherapies, the prognosis for KIRC remains poor, particularly for patients with advanced or metastatic disease. The five-year survival rate for patients with metastatic KIRC is notably low, often below 10% [4–6]. Given the clinical heterogeneity of KIRC and its aggressive progression, there is an urgent need to identify reliable biomarkers that can guide diagnosis, predict prognosis, and improve therapeutic outcomes. Traditional clinical and pathological parameters are often insufficient to accurately predict patient survival and treatment response. Therefore, the discovery of novel molecular markers is critical to advancing personalized treatment strategies.

The ubiquitin-specific protease (USP) family plays a pivotal role in regulating protein stability by removing ubiquitin from target proteins, influencing key cellular functions like cell cycle regulation, apoptosis, DNA repair, and signal transduction [7]. The USP family of deubiquitinating enzymes plays a crucial role in cancer progression by regulating the stability of key proteins involved in tumor growth and metastasis [8]. For example, USP2 and USP7 modulate p53 and MDM2, impacting cell survival and tumor development, while USP22 stabilizes c-Myc, driving cancer proliferation and metastasis [9–13]. Other USPs, such as USP15 and USP4, promote TGF-β signaling, facilitating epithelial-to-mesenchymal transition (EMT) and metastasis [14, 15]. USP9X and USP47 further influence EMT by stabilizing key proteins like SMAD4 and Snail, respectively [16–18]. Additionally, USP28 and USP10 contribute to tumorigenesis by regulating the DNA damage response and stabilizing p53 under stress conditions [19–21]. Together, these mechanisms highlight the central role of USPs in cancer development, positioning them as promising therapeutic targets.

In renal cancer, certain USPs have been shown to modulate sensitivity to therapies and influence tumor progression, positioning them as promising therapeutic targets [22–25]. For instance, USP8 has been implicated in the progression of renal cancer by stabilizing MUC12, a membrane-associated mucin that plays a critical role in maintaining epithelial integrity. Through deubiquitination, USP8 prevents MUC12 degradation, promoting tumor growth and malignancy [22]. USP37 contributes to cancer progression by deubiquitinating and stabilizing hypoxia-inducible factor 2α (HIF2α), a key driver of tumor adaptation to hypoxic conditions, thereby promoting tumor growth, angiogenesis, and metastasis [23]. Additionally, USP9X modulates autophagy and mTOR signaling by regulating the ubiquitination of the autophagy receptor p62. Loss of USP9X enhances the therapeutic efficacy of mTOR inhibitors, particularly in chromophobe renal cell carcinoma (chRCC), positioning USP9X as a potential target for improving treatment sensitivity in renal cancer [26]. However, the influence of USP35 on KIRC prognosis, its impact on immune therapy responses, and its role in tumor cell metastasis remain unclear. Further investigation is needed to elucidate how USP35 affects clinical outcomes and whether it plays a significant role in modulating immune responses or influencing tumor invasiveness in KIRC patients.

In this study, we aim to investigate the role of USP35 in KIRC by analyzing genomic data, expression patterns, and patient outcomes. Our goal is to elucidate the potential of USP35 as a prognostic biomarker and to explore its impact on tumor survival and resistance to treatment, offering insights into possible therapeutic interventions for KIRC. Additionally, we conducted in vitro experiments to validate our findings and further understand the mechanistic role of USP35 in KIRC progression and therapeutic response.

Methods

Data collection and processing

Publicly available datasets from The Cancer Genome Atlas (TCGA) and Genotype-Tissue Expression (GTEx) project were used for the analysis of USP35 expression, mutation, copy number variation (CNV), and DNA methylation in KIRC and other cancers. The datasets were accessed through the UCSC Xena browser and cBioPortal. For RNA sequencing data, transcript per million (TPM) values were used for gene expression normalization. Clinical data, including survival outcomes, were retrieved from the TCGA database for correlation analysis. Data preprocessing and normalization were conducted using R software (version 4.1.0), ensuring consistency across all datasets by applying standard bioinformatics protocols.

Gene expression analysis

Gene expression levels of USP35 and other genes in the USP family were quantified from RNA-seq data using TPM values. Differential expression analysis between tumor and normal tissues was conducted using the DESeq2 package in R. Results were adjusted for false discovery rate (FDR), and genes with an adjusted p-value < 0.05 were considered significant. Additional

validation was performed using the GTEx dataset to compare expression in normal tissues across multiple organs. Heatmaps and boxplots were generated to visualize gene expression patterns.

Mutation, CNV, and DNA Methylation analysis

Mutation data were extracted from the TCGA database and analyzed using the Maftools package in R. Mutation types such as missense, nonsense, and splice-site alterations were identified, and mutation frequencies across cancer subtypes were computed. CNV data were analyzed using GISTIC2.0, which identified significant focal amplifications and deletions. DNA methylation data, obtained from the Infinium Human Methylation 450 K BeadChip, were processed using the limma package in R to assess promoter methylation levels. Differential methylation analysis was conducted to evaluate the relationship between promoter methylation and USP35 gene expression.

Gene Set Enrichment Analysis (GSEA)

To investigate the biological processes associated with USP35 expression in KIRC, GSEA was performed using the GSEA software (Broad Institute). The RNA-seq data were ranked based on differential expression between high and low USP35 expression groups. Gene sets from the Molecular Signatures Database (MSigDB) were used to identify enriched pathways. The normalized enrichment score (NES) and FDR were calculated for each gene set, and pathways with an FDR < 0.05 were considered significantly enriched.

Cell Culture and Transfection

Human renal clear cell carcinoma (RCC) cell lines 786-O and ACHN were obtained from the American Type Culture Collection (ATCC). Cells were cultured in DMEM supplemented with 10% fetal bovine serum (FBS) and 1% penicillin–streptomycin. Cells were maintained at 37 °C with 5% CO2. For USP35 knockdown experiments, lentiviral vectors carrying shRNAs targeting USP35 (shUSP35-1, shUSP35-2, shUSP35-3) and a non-targeting control (shNC) were transfected into RCC cells using Lipofectamine 3000 (Invitrogen). Stable cell lines were selected using 2 μg/mL puromycin. Knockdown efficiency was confirmed via quantitative real-time PCR (qRT-PCR).

Quantitative Real-time PCR (qRT-PCR)

Total RNA was isolated from cells using the TRIzol reagent (Invitrogen). cDNA was synthesized using the PrimeScript RT reagent kit (Takara) following the manufacturer's protocol. qRT-PCR was performed on an ABI 7500 Fast Real-Time PCR system using SYBR Green Master Mix (Thermo Fisher Scientific). Relative USP35 mRNA levels were calculated using the 2^-ΔΔCt method, with GAPDH as the internal control. The primer sequences used for qRT-PCR are listed in Supplementary Table 1.

Colony Formation Assay

For the colony formation assay, transfected RCC cells were seeded into 6-well plates at a density of 500 cells per well. Cells were cultured for 14 days, fixed with 4% paraformaldehyde, and stained with 0.1% crystal violet. Colonies with more than 50 cells were counted under a microscope. Colony numbers were compared between control and USP35 knockdown groups.

CCK-8 Cell Proliferation Assay

Cell proliferation was assessed using the Cell Counting Kit-8 (CCK-8) assay (Dojindo). RCC cells transfected with either shUSP35 or shNC were seeded into 96-well plates at a density of 2,000 cells per well. Cell viability was measured at 24, 48, 72, and 96 h by adding 10 μL of CCK-8 reagent to each well, followed by incubation for 2 h. The absorbance was measured at 450 nm using a microplate reader (BioTek).

Wound Healing Assay

The wound healing assay was performed to evaluate cell migration. RCC cells were grown to confluence in 6-well plates, and a linear scratch was made using a sterile pipette tip. Cells were washed with PBS and cultured in serum-free medium. Wound closure was monitored at 0, 24, and 48 h using an inverted microscope. The percentage of wound closure was calculated and compared between groups.

Transwell Migration Assay

Transwell migration assays were performed using 8 μm pore size inserts (Corning). RCC cells were seeded in the upper chamber in serum-free medium, while medium containing 10% FBS was placed in the lower chamber. After 24 h, migrated cells on the lower surface of the membrane were fixed with methanol and stained with crystal violet. Migrated cells were counted in five randomly selected fields under a microscope.

Immunoblot Analysis

For Western blot analysis, RCC cells were lysed in RIPA buffer containing protease and phosphatase inhibitors (Roche). Protein concentrations were determined using the BCA protein assay kit (Thermo Fisher Scientific). Equal amounts of protein were separated on 10% SDS-PAGE gels and transferred to PVDF membranes. The membranes were blocked with 5% non-fat milk

and incubated with primary antibodies against USP35, N-cadherin, E-cadherin, and GAPDH overnight at 4 °C. Membranes were washed and incubated with HRP-conjugated secondary antibodies, and signals were detected using an enhanced chemiluminescence kit (Thermo Fisher Scientific).

Statistical Analysis

All statistical analyses were performed using GraphPad Prism (version 8.0) and R software (version 4.1.0). Data are presented as mean ± standard deviation (SD). Group comparisons were made using Student's t-test or one-way ANOVA. Survival analyses were conducted using Kaplan–Meier curves and log-rank tests. A p-value < 0.05 was considered statistically significant. Significance was defined as $^{*}p < 0.05$, $^{**}p < 0.01$, $^{***}p < 0.001$; ns indicates not significant.

Results

Multigene pan-cancer analysis of USP genes family

Mutiple USP gene family reveals significant expression differences across various cancer types, indicating their potential roles in tumor progression (Fig. 1A). The comprehensive pan-cancer differential expression analysis of the USP gene family across TCGA and GTEx datasets reveals widespread upregulation and downregulation of various USP genes in different cancer types. In the differential analysis, USP family genes show significant upregulation in cancers such as CHOL, DLBC, HNSC, LGG, PAAD, STAD and THYM (Fig. 1B). The univariate Cox survival analysis across multiple cancers reveals that different USP genes may act as either risk or protective factors, depending on the cancer type (Fig. 1C). We analyzed SNP data related to a specific gene set to detect the frequency and mutation types for each cancer subtype. UCEC, SKCM, STAD, and COAD exhibit the highest mutation frequencies among these cancers (Fig. 1D). Variant type analysis indicates that missense mutations are the most common, followed by nonsense mutations and splice site alterations, highlighting their potential role in driving tumorigenesis across these cancer types (Fig. 1E). Differences in promoter methylation levels among USP family genes are evident across various cancers, with notable variations in cancers such as KIRC, LUSC, and LIHC. These findings indicate the potential impact of epigenetic regulation on USP gene expression in different cancer types. The K-nearest neighbors (KNN) analysis highlights key USP genes associated with cancer progression. The CNV analysis suggest that both deletions and amplifications in USP genes may contribute to tumorigenesis and cancer progression in specific cancer subtypes (Supplementary Fig. 1). Collectively, our comprehensive analysis of the USP gene family reveals their diverse roles in cancer development, including differential expression, survival impact, genetic mutations, and epigenetic modifications, suggesting their potential as biomarkers across various cancer types.

Pan-Cancer analysis and prognostic implications of USP35 expression

Given the upregulation of USP35 in various cancers and its association with poor prognosis, we next explore its expression and prognostic significance across different cancers. The expression of USP35 is compared between normal and tumor tissues across multiple cancer types using TCGA data. In cancers such as BRCA, COAD, HNSC, KICH, KIRP, KIRC, LICH, LUAD, LUSC, READ and THCA, USP35 is notably overexpressed, suggesting its involvement in tumor progression. Pan-cancer analysis further highlights that USP35 expression is particularly elevated in liver, Brain Cancer, and endometrial/uterine cancers, while showing lower levels in lymphoma and Bile duct cancer (Fig. 2A-B). Samples were divided into USP35-high and USP35-low groups based on median expression. Regarding immune landscape, the USP35 high expression group was significantly enriched in inflammatory (C3) subtype, whereas the low expression group was enriched in wound healing (C1) and IFN-γ dominant (C2) subtypes (Fig. 2C). Understanding these subtypes is crucial as they suggest a potential interaction between USP35 expression and the tumor immune environment, potentially guiding personalized therapeutic strategies. USP35 expression is significantly influenced by copy number variations ($p < 0.001$) (Fig. 2D). Additionally, the ROC curve analysis reveals that USP35 shows significant diagnostic potential in cancers such as UCEC, STAD, and THCA, while moderate values are observed in BLCA and BRCA (Fig. 2E). Evaluation of USP35 dependency scores demonstrated varying degrees of essentiality across different cancer types, where higher scores reflect greater dependence on USP35 for cancer cell survival (Fig. 2F). Next, We evaluated hazard ratios (HR) with 95% confidence intervals across multiple cancer types for PFI (Progression-Free Interval), DSS (Disease-Specific Survival), and OS (Overall Survival). Notably, KIRC demonstrated significantly elevated hazard ratios across all three survival metrics (PFI: HR = 1.446, $p = 0.005$; DSS: HR = 2.052, $p < 0.001$; OS: HR = 2.006, $p < 0.001$) (F ig. 2G-I).. Taken together, USP35 is significantly overexpressed across multiple cancer types and associated with distinct immune subtypes, while its expression levels show prognostic value particularly in KIRC.

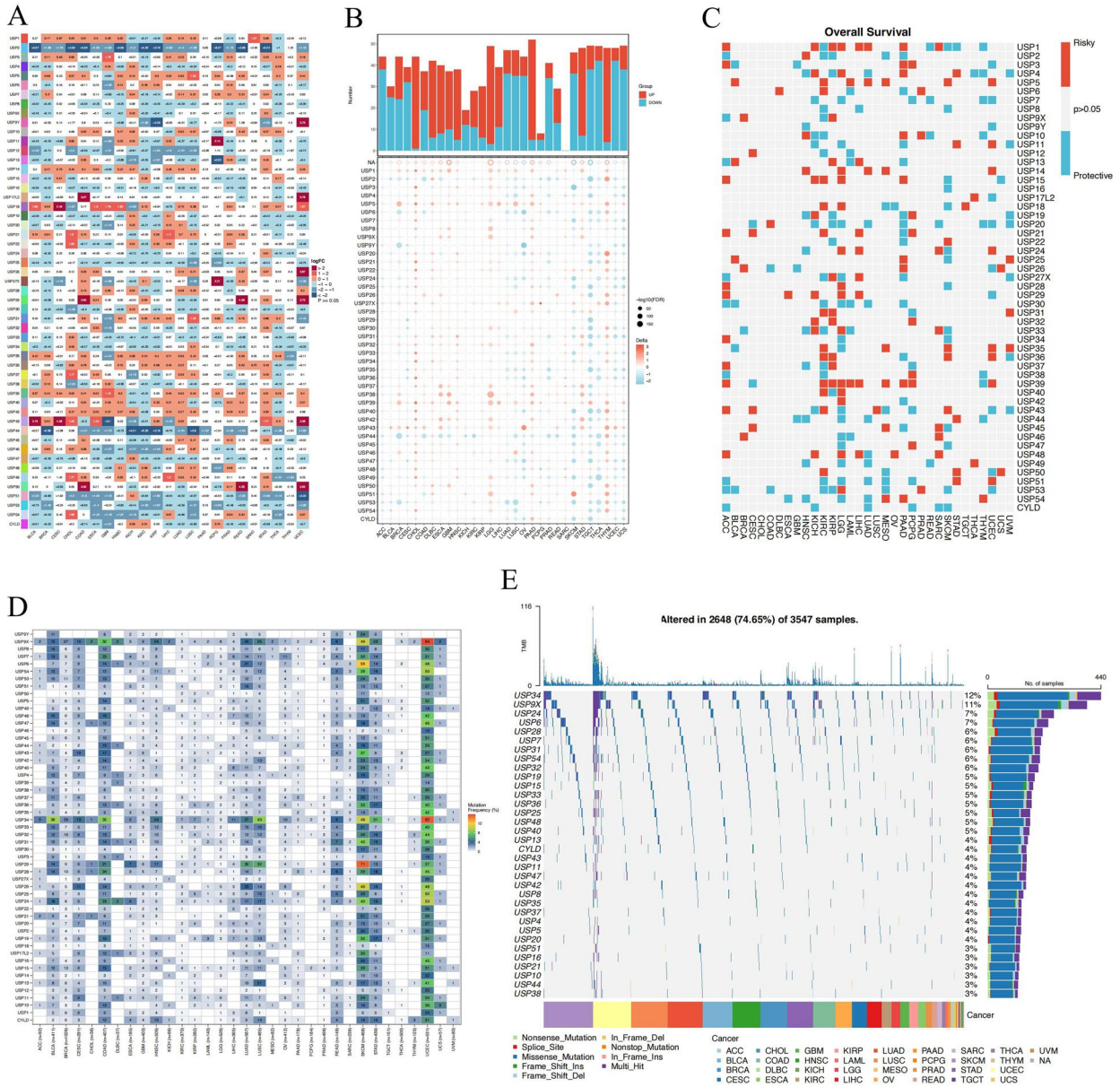

Fig. 1 Pan-cancer analysis of USP family genes. **A** Heatmap showing differential expression of USP genes across cancer types, with red indicating upregulation and blue indicating downregulation. **B** Bar chart illustrating the number of USP genes significantly upregulated (red) or downregulated (blue) in various cancers. **C** Univariate Cox analysis associating USP gene expression with overall survival, where red indicates risky and blue indicates protective roles. **D** Heatmap showing mutation frequencies of USP genes across cancers, with darker colors indicating higher mutation rates. **E** Waterfall plot displaying mutation types and frequencies of USP genes

(See figure on next page.)

Fig. 2 Pan-cancer analysis and clinical implications of USP35 expression. **A** USP35 expression comparison between tumor and normal tissues across various cancer types in TCGA data. **B** Paired analysis of USP35 expression in normal versus tumor tissues. **C** USP35 expression distribution across six molecular subtypes. C1 (wound healing), C2 (IFN-γ dominant), C3 (inflammatory), C4 (lymphocyte depleted), C5 (immunologically quiet), and C6 (TGF-β dominant). **D** Association between USP35 expression and copy number variations. **E** Diagnostic potential of USP35 across cancers. The x-axis represents the Area Under the ROC Curve (AUC) values, with the blue curve representing the TCGA-GTEx combined dataset and the red curve representing the TCGA dataset. **F** Based on the DepMap database, whole-gene CRISPR-Cas9 screening of the top 200 cell lines using CERES scores shows USP35 dependency across various cancer types. **G-I** Impact of USP35 expression on (**G**) progression-free interval (PFI), (**H**) disease-specific survival (DSS), and (**I**) overall survival (OS) in various cancers

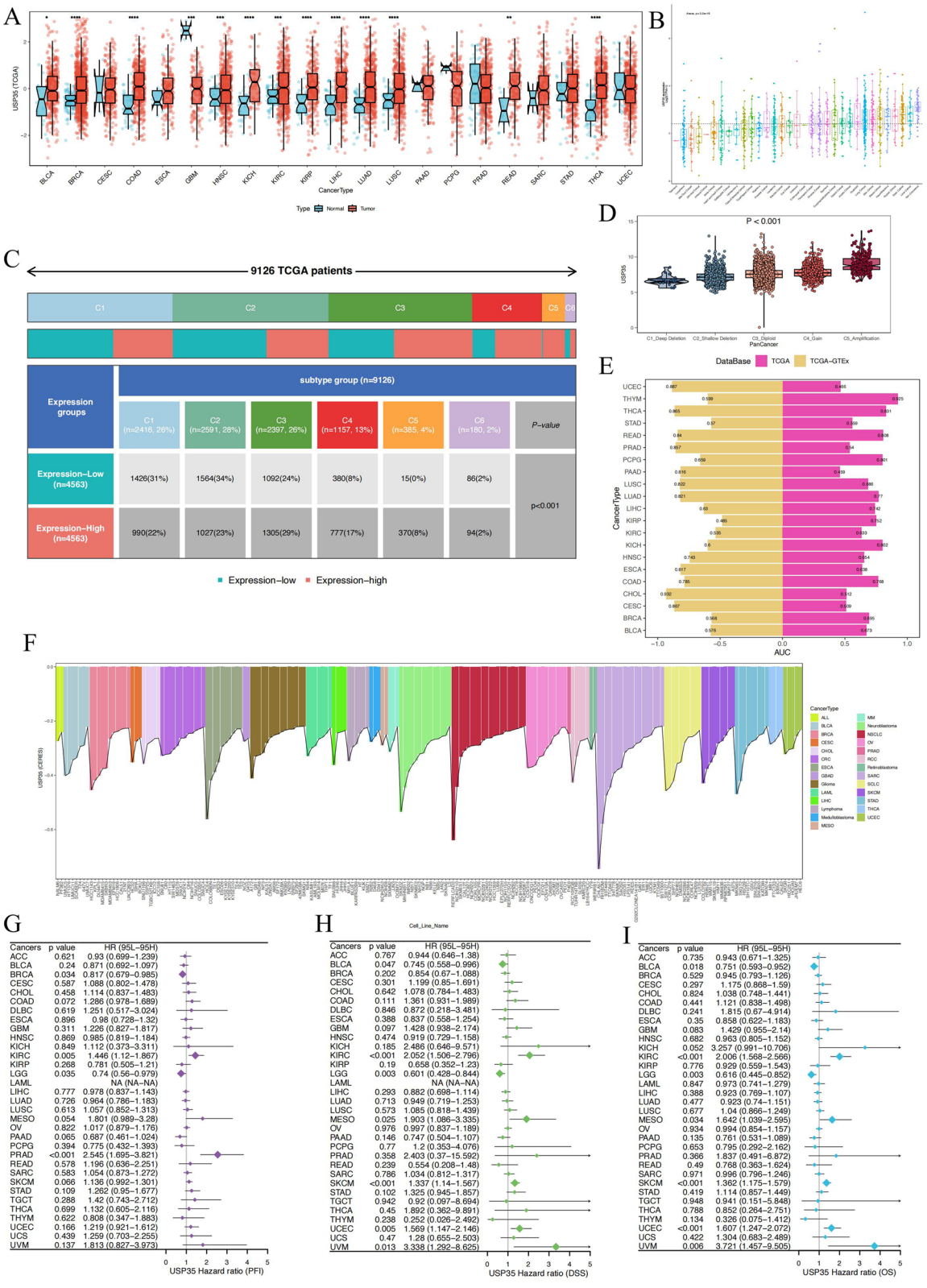

Fig. 2 (See legend on previous page.)

Correlation of USP35 expression with KIRC progression, clinical variables, and mutation profiles

Given that elevated USP35 expression is associated with prognosis in KIRC, we further investigated its potential contribution to tumor progression and patient outcomes. USP35 expression is significantly higher in tumor tissues compared to normal tissues, as shown in the TCGA_KIRC dataset (p = 6.5e-08) and the GSE167573 dataset (p = 0.062) (Fig. 3A). The analysis of USP35 expression across KIRC stages shows an increase from Stage I to Stage III, with a slight decrease in Stage IV, indicating its potential involvement in tumor progression (Fig. 3B). Additionally, USP35 expression differs significantly across stages in KIRC, with higher expression observed in later stages (p = 0.002) (Fig. 3C). USP35 expression in 512 TCGA patients shows that both the expression-high (84%) and expression-low (90%) groups are predominantly enriched in subtype C3. These differences are statistically significant (p = 0.049), indicating a correlation between USP35 expression and cancer subtypes (Fig. 3D). The distribution of clinical variables shows a correlation between USP35 expression and factors such as grade, TNM stage, and hemoglobin levels, suggesting its potential role in tumor progression and patient stratification (Fig. 3E). USP35 expression is associated with distinct mutation patterns, with VHL (59.5%), PBRM1 (50.2%), and TTN (21.1%) being the most frequently mutated genes, predominantly through missense mutations. Differences in mutation frequency between the expression groups suggest that USP35 expression may be linked to distinct mutation profiles in certain cancer-related genes (Fig. 3F). Analysis of USP35 in KIRC demonstrates its significant correlation with tumor progression, clinical features, and mutation patterns, supporting its potential as a prognostic biomarker.

Functional role of USP35 in KIRC

Next, we explored the functional role of USP35 in KIRC to further understand its contribution to tumor progression. USP35 expression shows significant positive correlations with processes such as apoptosis ($R = 0.3$, $p = 7.1e\text{-}13$), DNA damage ($R = 0.15$, $p = 0.00043$), DNA repair ($R = 0.11$, $p = 0.0084$), Differentiation ($R = 0.14$, $p = = 0.0015$), Proliferation ($R = 0.18$, $p = 3.2e-05$) and inflammation ($R = 0.17$, $p = 1e\text{-}04$). Conversely, negative correlations are observed with angiogenesis ($R = -0.088$, $p = 0.043$) and hypoxia ($R = -0.17$, $p = 6.2e\text{-}05$), suggesting USP35's varied roles across different oncogenic processes (Fig. 4A). Gene set variation analysis (GSVA) comparing high and low USP35 expression groups in KIRC reveals significant enrichment of metabolic pathways. High USP35 expression is associated with upregulation of glycerophospholipid metabolism, linoleic acid metabolism, and glycosaminoglycan biosynthesis, while low USP35 expression is linked to pathways such as nitrogen metabolism and purine metabolism. These findings highlight USP35's potential role in regulating metabolic processes in KIRC (Fig. 4B). USP35 expression shows strong correlations with several key cancer-related pathways, including apoptosis, DNA damage, and cell cycle regulation. In contrast, weaker correlations are observed with pathways like EMT and hormone signaling (Fig. 4C). Additionally, the analysis of SNV neoantigens across multiple cancer types reveals a significant positive correlation in LUAD and TGCT, while negative correlations are seen in cancers such as BRCA, THYM, LGG and PAAD. Tumors with a higher mutational burden may rely on USP35 to enhance immune evasion. (Fig. 4D). USP35 expression shows significant enrichment in several pathways. Notably, low expression is associated with processes such as the peroxisome pathway, ribosome function, and amino acid metabolism, while high expression is linked to immune-related pathways like cytokine-cytokine receptor interaction and primary immunodeficiency. This suggests a potential role for USP35 in both metabolic and immune regulation (Fig. 4E). Further analysis reveals that metabolic processes are enriched in low USP35 expression groups, while immune-related pathways show enrichment in high expression groups, indicating the diverse functional roles of USP35 in cancer biology (Fig. 4F). USP35 is involved in multiple cancer-related processes, playing a dual role in KIRC progression.

Cnv and methylation patterns of USP35 in KIRC

Epigenetic regulation controls the expression of USP35 in KIRC. The overall copy number variation analysis in the TCGA-KIRC cohort of 528 patients reveals that chr5 shows higher copy number gains, suggesting this region may be a characteristic feature of KIRC, while chr3 and chr6 exhibit lower GISTIC scores, indicating potential

(See figure on next page.)

Fig. 3 USP35 expression in KIRC and its correlation with clinical variables and mutations. **A** Comparison of USP35 expression between tumor and normal tissues in KIRC based on GSE167573 and TCGA datasets. **B** Median expression of USP35 across different KIRC stages. **C** USP35 expression levels across KIRC stages I to IV. **D** Distribution of USP35 expression across molecular subtypes of KIRC based on TCGA data. **E** Clinical variables associated with high and low USP35 expression, including factors like grade, TNM stage, and hemoglobin levels. **F** Mutation profiles of KIRC patients with high and low USP35 expression, showing the frequency and type of mutations in key cancer-related genes such as VHL, PBRM1, and TTN

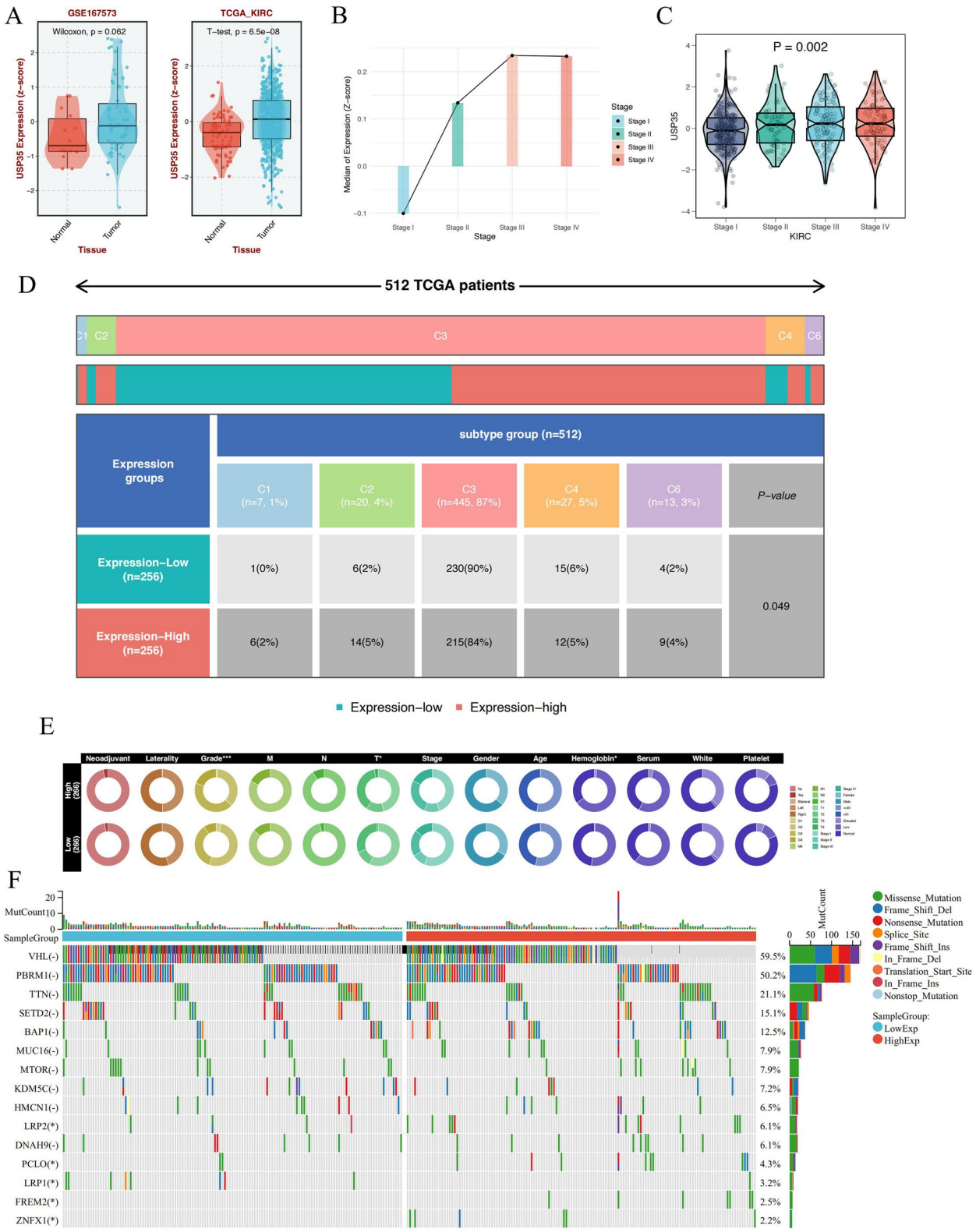

Fig. 3 (See legend on previous page.)

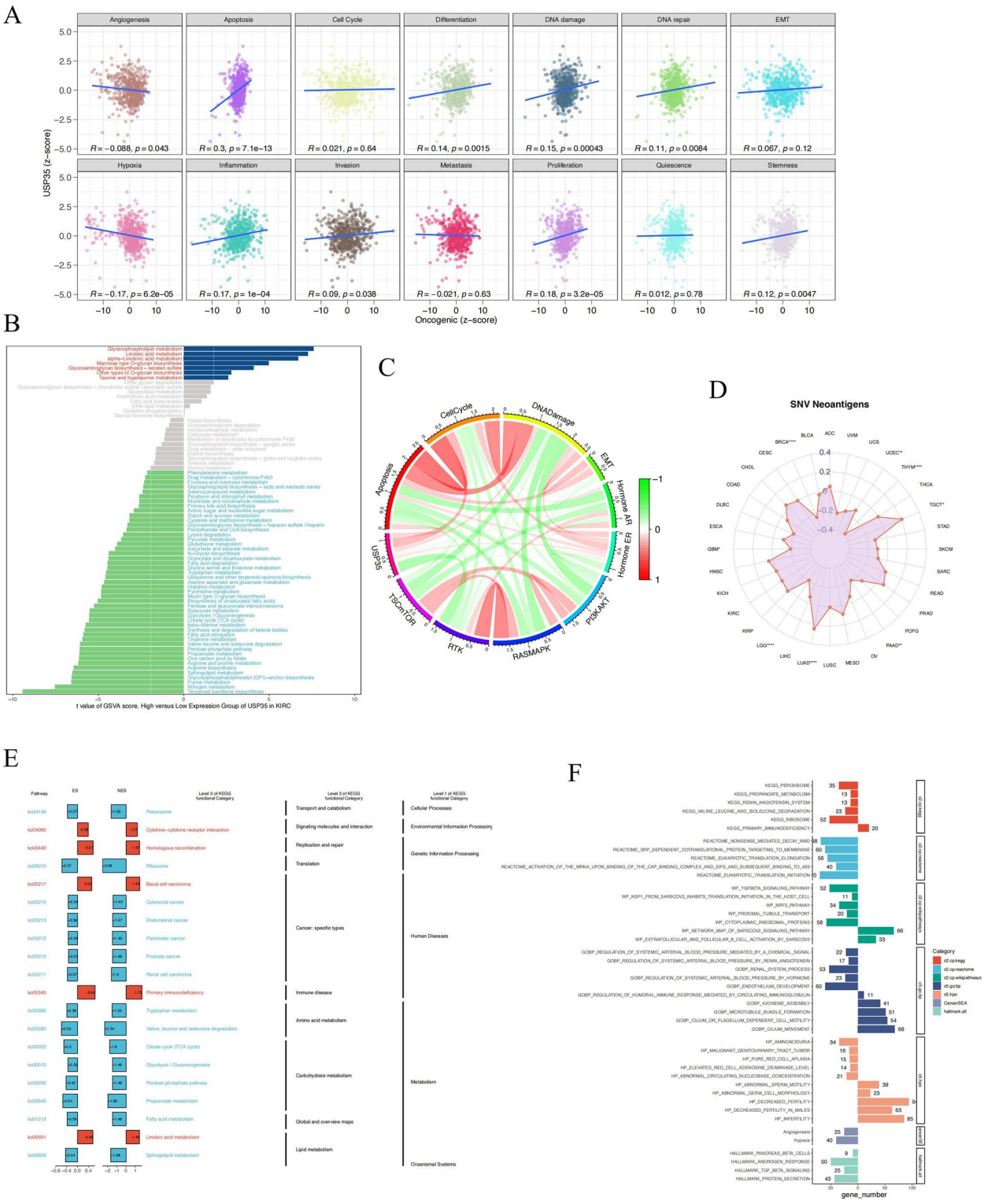

Fig. 4 Functional role of USP35 in KIRC and its involvement in oncogenic processes. **A** Correlation analysis of USP35 expression with various oncogenic processes. **B** GSVA comparing high and low USP35 expression groups in KIRC, highlighting metabolic pathway enrichment. **C** Circular plot illustrating the association between USP35 expression and several oncogenic pathways. **D** SNV Neoantigen burden correlation across cancer types in relation to USP35 expression. **E** GSEA on KEGG gene sets in pan-cancer, highlighting metabolic and immune-related differences between high and low USP35 expression groups. **F** Functional categorization of pathways associated with USP35 expression

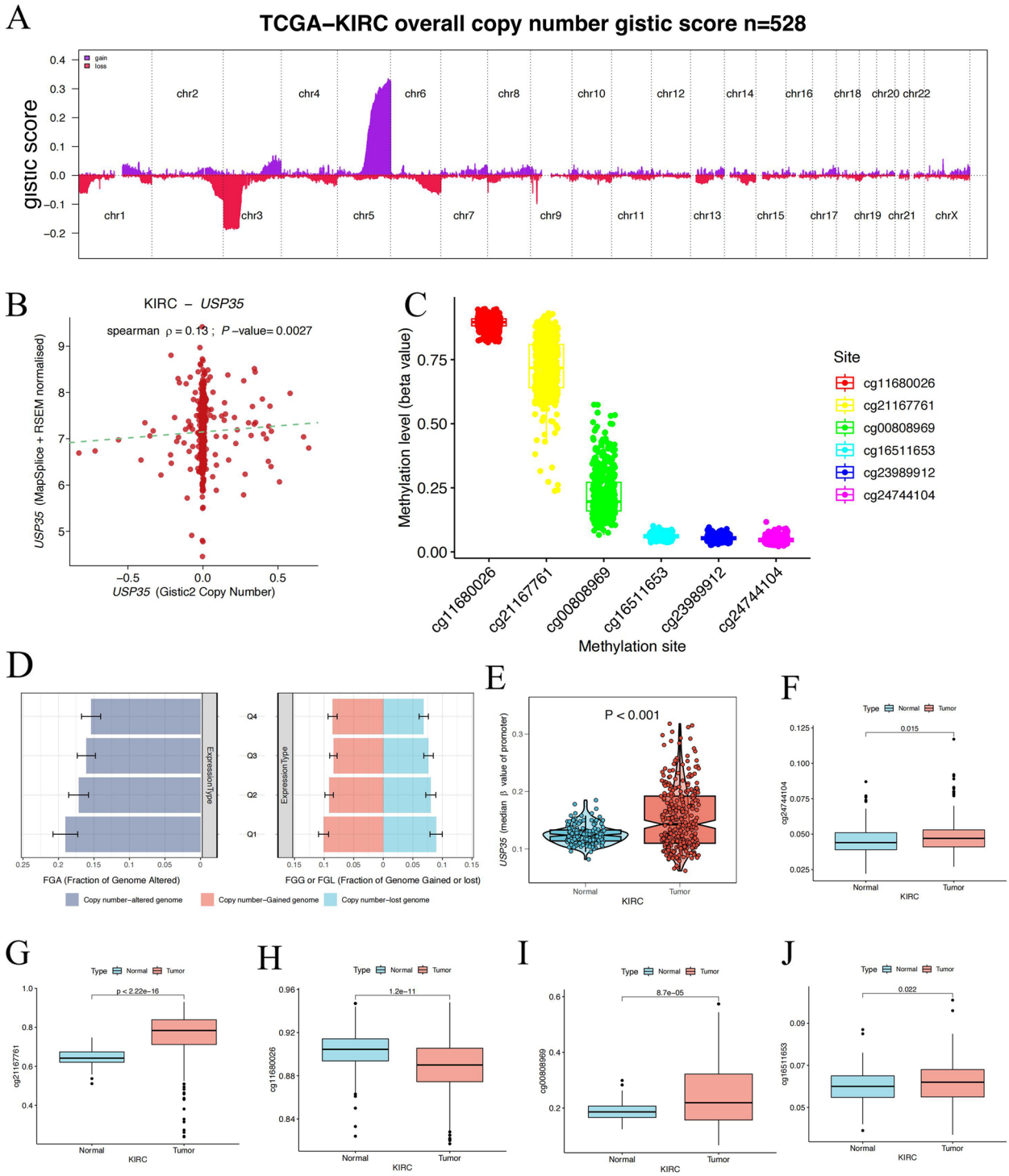

Fig. 5 Copy number variations and methylation analysis of USP35 in KIRC. **A** Visualization of USP35 copy number alterations across chromosomes in the TCGA-KIRC cohort. **B** Correlation between USP35 copy number and mRNA expression levels in KIRC. **C** Methylation analysis across six CpG sites for USP35. **D** Fraction of genome altered (FGA) and fraction of genome gained or lost (FGG/FGL) in relation to USP35 expression groups. **E** Comparison of USP35 promoter methylation levels between normal and tumor tissues. **F**-**J** Methylation levels at specific CpG sites (cg24744104, cg21167761, cg11680026, cg00808969, cg16511653) in normal versus tumor tissues

copy number losses (Fig. 5A). USP35 expression in KIRC shows statistically significant positive correlation with its copy number alterations (Spearman $\rho = 0.13$, $p = 0.0027$), indicating that increased copy number may contribute to higher expression levels (Fig. 5B). Additionally, methylation analysis across six CpG sites reveals distinct patterns, with cg11680026 showing the highest methylation levels, suggesting potential regulation of USP35 expression via epigenetic mechanisms (Fig. 5C). The analysis of the fraction of genome altered (FGA) and the fraction of genome gained or lost (FGG/FGL) shows a potential correlation between genomic changes and USP35 expression (Fig. 5D). Promoter methylation analysis of USP35 shows significantly higher methylation levels in KIRC tumor tissues compared to normal tissues ($p < 0.001$), indicating potential epigenetic regulation of USP35 in cancer (Fig. 5E). Analysis of multiple methylation sites reveals differential patterns between normal and tumor tissues in KIRC, with sites cg24744104, cg21167761, cg00808969, and cg16511653 showing increased methylation in tumors ($p < 0.05$), while cg11680026 exhibits decreased methylation (p = 1.2e-11) (Fig. 5F-J). The genomic and epigenetic analysis reveals that USP35 expression in KIRC is regulated through both copy number variations and differential methylation patterns.

Prognostic value of USP35 expression in KIRC

To investigate the prognostic value of USP35 in KIRC, we performed Cox regression analyses. In univariate analysis, several poor prognostic factors were identified, including higher grade, advanced TNM stage, lower hemoglobin, higher serum calcium, elevated platelet count, and increased USP35 expression. Multivariate analysis further revealed that gender, platelet qualitative and high USP35 expression were independent predictors of poor prognosis. Variables shown in bold indicate their 95% confidence intervals do not include 1, demonstrating statistical significance (Fig. 6A). The analysis demonstrates a non-linear relationship between USP35 expression and the hazard ratio (HR), with increased expression levels leading to a higher risk of poor outcomes (p-overall < 0.001, p-non-linear = 0.028) (Fig. 6B). The ROC curve analysis shows the predictive power of USP35 for 1-year, 5-year, and 10-year survival, with the AUC values of 0.617, 0.657, and 0.750, respectively, suggesting that USP35 expression may have a significant impact on prognosis (Fig. 6C). The meta-analysis of multiple studies reveals that USP35 expression is associated with a significantly higher HR for poor outcomes across various cohorts (Fig. 6D). Survival analysis in KIRC reveals that high USP35 expression is associated with significantly poorer DSS ($p < 0.001$), PFS ($p = 0.002$), and OS ($p < 0.001$) compared to low expression (Fig. 6E-G). Further stratification of patients into quartiles by USP35 expression levels (Q1-Q4) confirms that highest expression correlates with worst survival outcomes across all three measures (DSS, $p < 0.001$; PFI, $p = 0.006$; OS, $p < 0.001$), reinforcing its potential as a negative prognostic marker (Fig. 6H-J). Both univariate and multivariate analyses confirm USP35 as an independent prognostic factor in KIRC, with high expression consistently associated with poor survival outcomes.

USP35 expression correlates with immune regulation and diverse anti-cancer drugs response

In order to explore the potential impact of USP35 on immune regulation and its relevance to immunotherapy efficacy, we examined its expression in relation to various immune factors and drug sensitivity. USP35 expression in KIRC is associated with various immune factors, indicating a role in immune response regulation (Fig. 7A). USP35 shows significant correlations with various steps of the cancer immunity cycle, including a positive correlation with steps involved in immune cell recruitment, such as $CD4^+$ T cell, $CD8^+$ T cell and macrophage recruiting (Fig. 7B). USP35 expression is correlated with a broad range of immune-related genes, spanning co-stimulatory and co-inhibitory molecules, ligands, receptors, and cell adhesion molecules (Fig. 7C). USP35 expression is associated with various immune response and genomic state factors (Fig. 7D). Further, we explored the relationship between USP 35 expression level and drug sensitivity in different datasets. In the CTRP dataset, USP35 was significantly related to the effectiveness of drugs like lapatinib, ciclopirox, fluorouracil, afatinib, and canertinib, suggesting that higher expression may

(See figure on next page.)

Fig. 6 USP35 related prognostic analysis in KIRC. **A** Univariate and multivariate Cox regression analysis for USP35 expression and other clinical factors in KIRC. **B** Non-linear relationship between USP35 expression and hazard ratio (HR), showing increased risk with higher USP35 expression levels. **C** ROC curve analysis of USP35 expression predicting 1-year, 5-year, and 10-year survival in KIRC patients. **D** Meta-analysis showing the association of USP35 expression with hazard ratios across multiple datasets. **E**–**G** Kaplan–Meier survival curves showing the correlation between high and low USP35 expression with disease-specific survival (**E**), progression-free interval (**F**), and overall survival (**G**) in KIRC. **H**-**J** Stratified analysis of USP35 expression into quartiles (Q1-Q4), showing significant differences in disease-specific survival (**H**), progression-free interval (**I**), and overall survival (**J**)

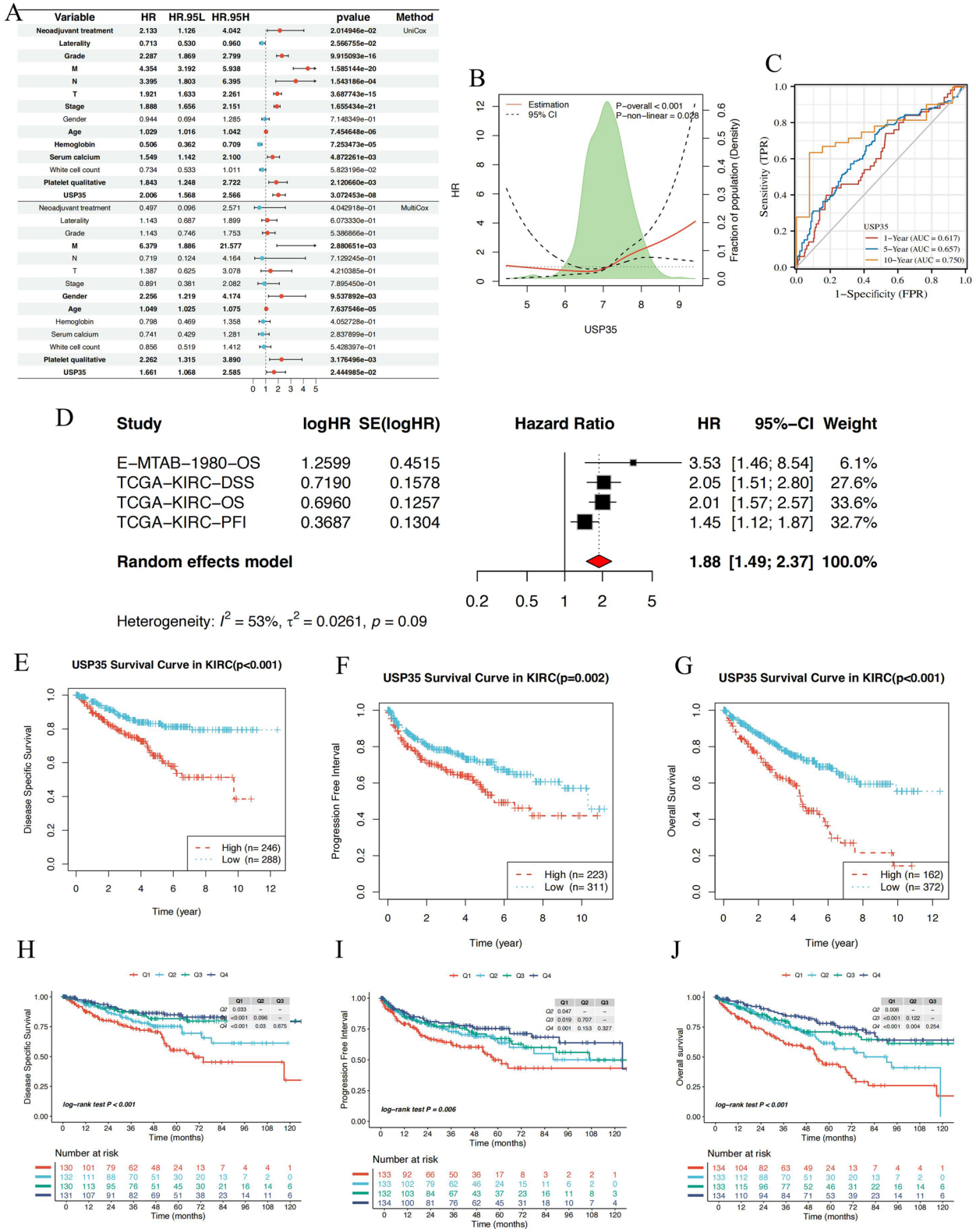

Fig. 6 (See legend on previous page.)

correlate with increased sensitivity to these drugs. In the PRISM dataset, USP35 was linked to sensitivity to drugs such as taselisib, afatinib, and repsox, with similar patterns observed in the GDSC1 dataset where USP35 expression is connected to drugs like GSK690693, PHA-793887, and NPK76-II-72–1(Fig. 7E-G). USP35 expression levels are associated with sensitivity to several drugs. High USP35 expression correlates with greater sensitivity to both Paclitaxel and Bosutinib ($p=0.0097$ and $p=3.8e-06$ respectively) (F ig. 7H-I). Additionally, low USP35 expression demonstrates higher sensitivity to Lapatinib compared to the high USP35 group ($p=9.9e-12$) (Fig. 7J). In multiple cohorts, USP35 expression is significantly higher in non-responders to anti-PD-L1 therapy (Wolf cohort: $p=0.0029$; Mvigor210 cohort: $p=0.03$), while showing no significant difference in anti-CTLA-4-treated patients (Nathanson cohort: $p=0.07$) (Fig. 7K). Additionally, in the melanoma cohort (GSE78220), USP35 expression was significantly elevated in non-responders ($p=0.025$) (Fig. 7L), and the ROC curve analysis revealed that USP35 expression has predictive potential with an AUC of 0.749 (95% CI: 0.554–0.918) (Fig. 7N), indicating that USP35 may serve as a potential biomarker for predicting response to immunotherapy. Collectively, our analysis demonstrates that USP35 plays a crucial role in immune regulation and drug response, with its expression levels potentially serving as a predictive biomarker for both chemotherapy and immunotherapy outcomes.

In vitro knockdown of USP35 suppresses KIRC cell proliferation, migration, and EMT

In continuation of our investigation into the role of USP35 in KIRC, we conducted a series of in vitro experiments to assess its effects on cell proliferation, migration, and oncogenic pathways. Knockdown of USP35 was confirmed through qPCR, which showed significantly reduced mRNA levels in all three shUSP35 knockdown groups compared to the control (NC) group ($p<0.01$) (Fig. 8A). Colony formation assays revealed that silencing USP35 led to a significant decrease in the number of colonies formed by KIRC cells, indicating reduced cell proliferation (Fig. 8B). The CCK-8 cell viability assay further demonstrated that cells with USP35 knockdown exhibited a significantly slower growth rate compared to the control group at multiple time points ($p<0.001$) (Fig. 8C). Gene set enrichment analysis (GSEA) revealed that silencing USP35 significantly impacted several pathways, including processes such as epithelial-mesenchymal transition (EMT), coagulation, angiogenesis, and TNF-alpha signaling via NF-kB, which are crucial for tumor progression (Fig. 8D). Additionally, wound healing assays showed that USP35 knockdown significantly inhibited the migratory ability of KIRC cells, as indicated by reduced wound closure after 48 h compared to the control group (Fig. 8E). These results suggest that USP35 may play a role in promoting KIRC cell proliferation and related oncogenic pathways. Silencing of USP35 significantly reduces wound healing capacity, with the wound closure rate decreasing from 80% to approximately 60% ($p<0.05$) (Fig. 8F). Additionally, migration assay results show a marked reduction in the number of migrated cells in the USP35-silenced group, dropping from around 100 to about 50 cells ($p<0.0001$) (Fig. 8G-H). These findings indicate that USP35 knockdown significantly inhibits the wound healing and migration abilities of KIRC cells. Silencing USP35 significantly reduced N-cadherin levels and increased E-cadherin expression ($p<0.01$), indicating its role in regulating EMT in KIRC cells (F ig. 8I-J). In vitro experiments demonstrate that USP35 knockdown inhibits KIRC cell proliferation and migration while modulating EMT-related protein expression, confirming its functional importance in KIRC progression.

Discussion

KIRC is a particularly aggressive subtype of renal carcinoma, with a high mortality rate and poor prognosis for advanced stages. Current clinical markers often fall short in predicting outcomes or guiding treatment, highlighting the urgent need for novel biomarkers to improve patient management [4]. Our study identifies USP35 as a significant driver of tumor progression in KIRC. We found that USP35 is overexpressed in tumor tissues and correlates with advanced clinical stages and poorer survival outcomes. These findings align with recent studies where USP35 has been implicated in promoting cancer progression across several types of cancer, contributing to both tumor growth and therapeutic resistance [27, 28].

(See figure on next page.)

Fig. 7 USP35 expression correlates with immune regulation and anti-cancer drug responses. **A** Correlation between USP35 expression and immune-related genes. **B** Association of USP35 with the cancer immunity cycle. **C** Correlations between USP35 expression and immune regulatory molecules. **D** Relationship between USP35 expression and immune response/genomic state features. **E**–**G** Drug sensitivity analysis in (**E**) CTRP, (**F**) PRISM, and (**G**) GDSC1 datasets. **H**-**J** Analysis of (**H**) Paclitaxel, (**I**) Bosutinib, and (**J**) Lapatinib sensitivity between high and low USP35 expression groups. **K** USP35 expression in immune checkpoint inhibitor cohorts. **L** USP35 expression in responders vs. non-responders in melanoma. **N** ROC curve for predicting immunotherapy response based on USP35 expression

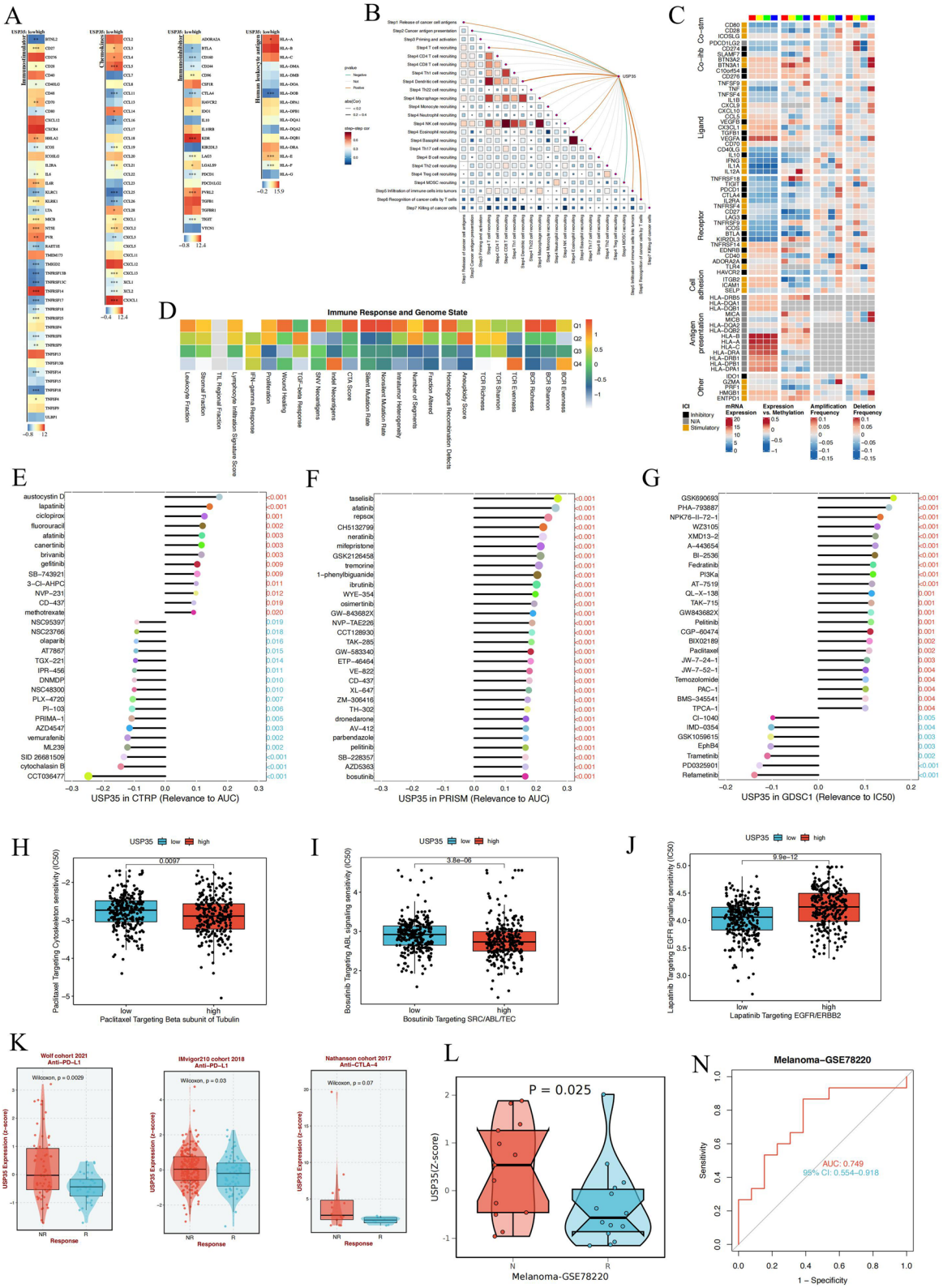

Fig. 7 (See legend on previous page.)

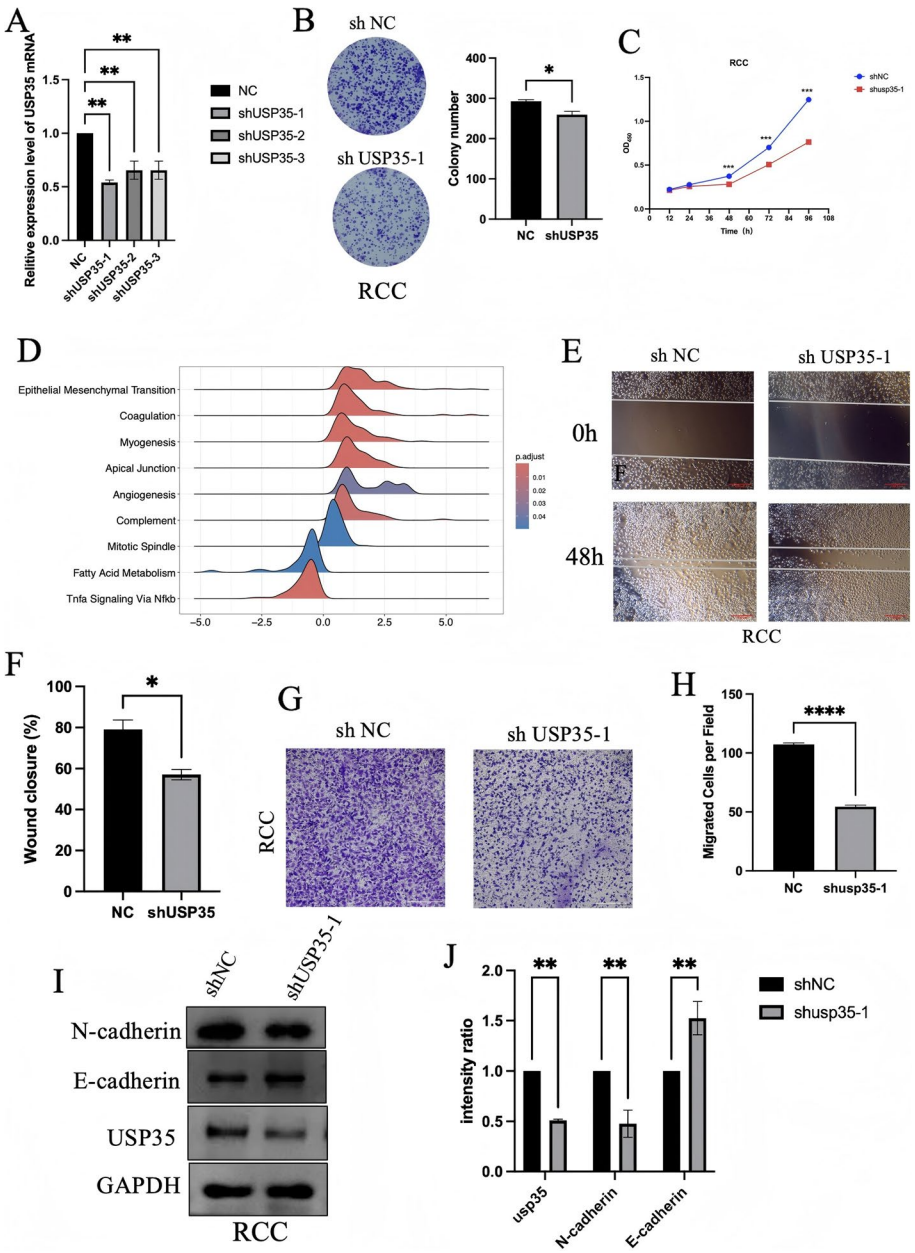

Fig. 8 USP35 knockdown impacts proliferation, migration, and EMT in RCC cells. **A** USP35 mRNA levels in knockdown and control groups. **B** Colony formation in RCC cells. **C** Cell viability over time. **D** Enrichment of oncogenic pathways. **E** Wound healing assay results. **F** Wound closure quantification. **G**-**H** Migration assay results. **I** N-cadherin and E-cadherin levels post-knockdown. **J** Protein intensity quantification. All in vitro experiments were performed with at least three independent replicates

Genomic alterations, particularly CNV, influence USP35 expression, with amplifications leading to higher levels. Importantly, USP35 emerged as a negative prognostic marker in KIRC. High USP35 expression was associated with poorer outcomes in DSS, PFI, and OS. This is consistent with studies in NSCLC, where elevated USP35 levels predict unfavorable prognosis by promoting tumor survival under stress conditions [29]. Functionally, USP35 appears to promote tumor cell survival by stabilizing proteins involved in apoptosis, DNA damage response, and cell cycle regulation. GSEA revealed that high USP35 expression is linked to upregulated metabolic pathways, such as glycerophospholipid and linoleic acid metabolism. Metabolic reprogramming is a hallmark of cancer, supporting rapid cell proliferation and survival [30]. In CRC, USP35 stabilizes FUCA1, enhancing glycosylation

and DNA repair, which contributes to chemoresistance [31].

Additionally, our study found that USP35 modulates immune responses in KIRC. Its expression correlates with immune cell recruitment and neoantigen presentation, suggesting a role in immune evasion and shaping the tumor microenvironment. This observation is in line with reports that deubiquitinating enzymes like USP35 can regulate immune signaling pathways and affect immune cell infiltration [32, 33]. Notably, higher USP35 expression was observed in non-responders to anti-PD-L1 immunotherapy, indicating that USP35 may contribute to immunotherapy resistance. This finding is particularly relevant, as immune checkpoint inhibitors are a cornerstone in advanced KIRC treatment [34, 35]. In terms of drug sensitivity, higher USP35 expression in KIRC correlated with increased sensitivity to therapeutic agents, including paclitaxel, bosutinib, and lapatinib. This contrasts with some studies in other cancers where USP35 contributes to chemotherapy resistance—for example, in lung cancer, USP35 stabilizes ferroportin, supporting tumor growth and conferring resistance to chemotherapy [36]. This discrepancy suggests that USP35's influence on drug sensitivity may be context-dependent, varying across different cancer types and treatments.

Our knockdown experiments provided direct evidence of USP35's functional importance in KIRC. Silencing USP35 resulted in significantly reduced cell proliferation, migration, and epithelial-mesenchymal transition (EMT). The decrease in N-cadherin and increase in E-cadherin levels following USP35 knockdown indicate that USP35 actively promotes EMT, facilitating tumor invasion and metastasis. Similar effects have been observed in breast cancer, where USP35 enhances tumorigenesis by stabilizing estrogen receptor α (ERα), leading to increased proliferation and metastasis [37]. ERα plays a crucial role in regulating EMT by influencing the expression of EMT-related genes and transcription factors; its activation can downregulate epithelial markers like E-cadherin and upregulate mesenchymal markers such as N-cadherin and vimentin, thus promoting EMT and enhancing metastatic potential [38, 39]. Therefore, USP35 may influence EMT and metastasis in KIRC through its deubiquitinating activity by stabilizing key proteins like ERα that regulate these processes, although further research is needed to elucidate these pathways.

Overall, our findings position USP35 as both a prognostic biomarker and a promising therapeutic target in KIRC. Targeting USP35 could potentially inhibit tumor progression and overcome resistance to therapy. The development of USP inhibitors has shown promise in cancer therapy, with some advancing to clinical trials [40, 41]. Inhibitors targeting other USPs, such as USP7 and USP14, have demonstrated efficacy in preclinical models by disrupting protein degradation pathways and impairing cancer cell survival [42, 43]. These advancements highlight the potential of developing specific USP35 inhibitors for KIRC treatment. However, our study has limitations. The lack of in vivo validation and a detailed understanding of the mechanisms underlying USP35's influence on immune responses warrant further investigation. Future studies should focus on elucidating the molecular pathways mediated by USP35 in KIRC, particularly its interactions with the immune system and impact on therapeutic responses. This could pave the way for developing targeted therapies that improve patient outcomes by overcoming treatment resistance.

Supplementary Information

The online version contains supplementary material available at https://doi.org/10.1186/s12885-025-13964-w.

Supplementary Material 1.

Supplementary Material 2.

Authors' contributions

Y.G. and P.W., together with X.Y., conceptualized the study. Y.G. and S.M. developed the methodology. Z.L. curated the data and conducted formal analysis. Z.L., Z.S., and X.Y. reviewed and edited the manuscript. Z.Z. conducted the investigation, created visualizations, and performed validation. W.Z. provided resources, software, and conducted data analysis. S.M. and Z.S. administered the project. Y.G., Z.S., and X.Y. provided supervision. Y.G. wrote the original draft. P.W. provided resources, and together with X.Y., secured funding for the project. All authors reviewed the manuscript.

Funding

This work was supported in part by grants from "Experimental Animal" Fund of Shanghai Science and Technology Commission, Grant No. 22140903800.

Data availability

The data used in this study are publicly available from The Cancer Genome Atlas (TCGA) at [https://portal.gdc.cancer.gov/] and other relevant repositories. Additional data generated during the study, including processed datasets and analysis scripts, are available from the corresponding author upon reasonable request. All data comply with ethical and privacy standards.

Declarations

Ethical approval and consent to participate

This study utilized publicly available datasets from The Cancer Genome Atlas (TCGA) and other databases, which do not require ethical approval as per the guidelines established by the Declaration of Helsinki and the U.S. Department of Health and Human Services regulations.

Consent for publication

Consent for publication is not applicable.

Competing interests

The authors declare no competing interests.

Author details

[1]Department of Urology, School of Medicine, Shanghai Tenth People'S Hospital, Tongji University, Shanghai, China. [2]Urologic Cancer Institute, Tongji University School of Medicine, Shanghai, China. [3]School of Medicine, Tongji University, Shanghai 200092, China. [4]Department of Colorectal Surgery, Fudan University Shanghai Cancer Center, Shanghai, China. [5]Laboratory of Ruijin

Hospitalaffiliated to, Wuxi Branchaq, Shanghai Jiaotong University School of Medicine, Wuxi, Jiangsu, China.

Received: 1 November 2024 Accepted: 18 March 2025
Published online: 05 April 2025

References

1. Bray, F., Laversanne, M., Sung, H., Ferlay, J., Siegel, R.L., Soerjomataram, I., and Jemal, A. (2024). Global cancer statistics 2022: GLOBOCAN estimates of incidence and mortality worldwide for 36 cancers in 185 countries. CA: A Cancer Journal for Clinicians *74*, 229–263. https://doi.org/10.3322/caac.21834.
2. Motzer RJ, Bander NH, Nanus DM. Renal-cell carcinoma. N Engl J Med. 1996;335:865–75. https://doi.org/10.1056/nejm199609193351207.
3. Bahadoram, S., Davoodi, M., Hassanzadeh, S., Bahadoram, M., Barahman, M., and Mafakher, L. (2022). Renal cell carcinoma: an overview of the epidemiology, diagnosis, and treatment. G Ital Nefrol *39*.
4. Hsieh JJ, Purdue MP, Signoretti S, Swanton C, Albiges L, Schmidinger M, Heng DY, Larkin J, Ficarra V. Renal cell carcinoma. Nat Rev Dis Primers. 2017;3:17009. https://doi.org/10.1038/nrdp.2017.9.
5. Liu, D., Wu, G., Wang, S., Zheng, X., and Che, X. (2024). Evaluating the Role of Neddylation Modifications in Kidney Renal Clear Cell Carcinoma: An Integrated Approach Using Bioinformatics, MLN4924 Dosing Experiments, and RNA Sequencing. Pharmaceuticals (Basel) *17*. https://doi.org/10.3390/ph17050635.
6. Zhang G, Chen X, Fang J, Tai P, Chen A, Cao K. Cuproptosis status affects treatment options about immunotherapy and targeted therapy for patients with kidney renal clear cell carcinoma. Front Immunol. 2022;13:954440. https://doi.org/10.3389/fimmu.2022.954440.
7. Cruz, L., Soares, P., and Correia, M. (2021). Ubiquitin-Specific Proteases: Players in Cancer Cellular Processes. Pharmaceuticals (Basel) *14*. https://doi.org/10.3390/ph14090848.
8. Young M-J, Hsu K-C, Lin TE, Chang W-C, Hung J-J. The role of ubiquitin-specific peptidases in cancer progression. J Biomed Sci. 2019;26:42. https://doi.org/10.1186/s12929-019-0522-0.
9. Yi J, Tavana O, Li H, Wang D, Baer RJ, Gu W. Targeting USP2 regulation of VPRBP-mediated degradation of p53 and PD-L1 for cancer therapy. Nat Commun. 2023;14:1941. https://doi.org/10.1038/s41467-023-37617-3.
10. Stevenson LF, Sparks A, Allende-Vega N, Xirodimas DP, Lane DP, Saville MK. The deubiquitinating enzyme USP2a regulates the p53 pathway by targeting Mdm2. Embo j. 2007;26:976–86. https://doi.org/10.1038/sj.emboj.7601567.
11. Qi SM, Cheng G, Cheng XD, Xu Z, Xu B, Zhang WD, Qin JJ. Targeting USP7-Mediated Deubiquitination of MDM2/MDMX-p53 Pathway for Cancer Therapy: Are We There Yet? Front Cell Dev Biol. 2020;8:233. https://doi.org/10.3389/fcell.2020.00233.
12. Sheng Y, Saridakis V, Sarkari F, Duan S, Wu T, Arrowsmith CH, Frappier L. Molecular recognition of p53 and MDM2 by USP7/HAUSP. Nat Struct Mol Biol. 2006;13:285–91. https://doi.org/10.1038/nsmb1067.
13. Kim D, Hong A, Park HI, Shin WH, Yoo L, Jeon SJ, Chung KC. Deubiquitinating enzyme USP22 positively regulates c-Myc stability and tumorigenic activity in mammalian and breast cancer cells. J Cell Physiol. 2017;232:3664–76. https://doi.org/10.1002/jcp.25841.
14. Eichhorn PJ, Rodón L, Gonzàlez-Juncà A, Dirac A, Gili M, Martínez-Sáez E, Aura C, Barba I, Peg V, Prat A, et al. USP15 stabilizes TGF-β receptor I and promotes oncogenesis through the activation of TGF-β signaling in glioblastoma. Nat Med. 2012;18:429–35. https://doi.org/10.1038/nm.2619.
15. Zhang L, Zhou F, Drabsch Y, Gao R, Snaar-Jagalska BE, Mickanin C, Huang H, Sheppard KA, Porter JA, Lu CX, ten Dijke P. USP4 is regulated by AKT phosphorylation and directly deubiquitylates TGF-β type I receptor. Nat Cell Biol. 2012;14:717–26. https://doi.org/10.1038/ncb2522.
16. Dupont S, Mamidi A, Cordenonsi M, Montagner M, Zacchigna L, Adorno M, Martello G, Stinchfield MJ, Soligo S, Morsut L, et al. FAM/USP9x, a deubiquitinating enzyme essential for TGFbeta signaling, controls Smad4 monoubiquitination. Cell. 2009;136:123–35. https://doi.org/10.1016/j.cell.2008.10.051.
17. Wu Y, Yu X, Yi X, Wu K, Dwabe S, Atefi M, Elshimali Y, Kemp KT 2nd, Bhat K, Haro J, et al. Aberrant Phosphorylation of SMAD4 Thr277-Mediated USP9x-SMAD4 Interaction by Free Fatty Acids Promotes Breast Cancer Metastasis. Cancer Res. 2017;77:1383–94. https://doi.org/10.1158/0008-5472.Can-16-2012.
18. Choi BJ, Park SA, Lee SY, Cha YN, Surh YJ. Hypoxia induces epithelial-mesenchymal transition in colorectal cancer cells through ubiquitin-specific protease 47-mediated stabilization of Snail: A potential role of Sox9. Sci Rep. 2017;7:15918. https://doi.org/10.1038/s41598-017-15139-5.
19. Lambrus BG, Daggubati V, Uetake Y, Scott PM, Clutario KM, Sluder G, Holland AJ. A USP28-53BP1-p53-p21 signaling axis arrests growth after centrosome loss or prolonged mitosis. J Cell Biol. 2016;214:143–53. https://doi.org/10.1083/jcb.201604054.
20. Fong, C.S., Mazo, G., Das, T., Goodman, J., Kim, M., O'Rourke, B.P., Izquierdo, D., and Tsou, M.F. (2016). 53BP1 and USP28 mediate p53-dependent cell cycle arrest in response to centrosome loss and prolonged mitosis. Elife *5*. https://doi.org/10.7554/eLife.16270.
21. Yuan J, Luo K, Zhang L, Cheville JC, Lou Z. USP10 regulates p53 localization and stability by deubiquitinating p53. Cell. 2010;140:384–96. https://doi.org/10.1016/j.cell.2009.12.032.
22. Zhang W, Zheng Z, Wang K, Mao W, Li X, Wang G, Zhang Y, Huang J, Zhang N, Wu P, et al. piRNA-1742 promotes renal cell carcinoma malignancy by regulating USP8 stability through binding to hnRNPU and thereby inhibiting MUC12 ubiquitination. Exp Mol Med. 2023;55:1258–71. https://doi.org/10.1038/s12276-023-01010-3.
23. Hong K, Hu L, Liu X, Simon JM, Ptacek TS, Zheng X, Liao C, Baldwin AS, Zhang Q. USP37 promotes deubiquitination of HIF2α in kidney cancer. Proc Natl Acad Sci U S A. 2020;117:13023–32. https://doi.org/10.1073/pnas.2002567117.
24. Meng, X., Xiong, Z., Xiao, W., Yuan, C., Wang, C., Huang, Y., Tong, J., Shi, J., Chen, Z., Liu, C., et al. (2020). Downregulation of ubiquitin-specific protease 2 possesses prognostic and diagnostic value and promotes the clear cell renal cell carcinoma progression. Ann Transl Med *8*, 319. https://doi.org/10.21037/atm.2020.02.141.
25. Wang S, Wang T, Zhang X, Cheng S, Chen C, Yang G, Wang F, Wang R, Zhang Q, Yang D, et al. The deubiquitylating enzyme USP35 restricts regulated cell death to promote survival of renal clear cell carcinoma. Cell Death Differ. 2023;30:1757–70. https://doi.org/10.1038/s41418-023-01176-3.
26. Roldán-Romero JM, Valdivia C, Santos M, Lanillos J, Maroto P, Anguera G, Calsina B, Martinez-Montes A, Monteagudo M, Mellid S, et al. Deubiquitinase USP9X loss sensitizes renal cancer cells to mTOR inhibition. Int J Cancer. 2023;153:1300–12. https://doi.org/10.1002/ijc.34575.
27. Liu C, Chen Z, Ding X, Qiao Y, Li B. Ubiquitin-specific protease 35 (USP35) mediates cisplatin-induced apoptosis by stabilizing BIRC3 in non-small cell lung cancer. Lab Invest. 2022;102:524–33. https://doi.org/10.1038/s41374-021-00725-z.
28. Zhang D, Li J, Zhang C, Xue J, Li P, Shang K, Zhang X, Lang B. The deubiquitinating enzyme USP35 regulates the stability of NRF2 protein. Open Life Sci. 2024;19:20220935. https://doi.org/10.1515/biol-2022-0935.
29. Wang W, Wang M, Xiao Y, Wang Y, Ma L, Guo L, Wu X, Lin X, Zhang P. USP35 mitigates endoplasmic reticulum stress-induced apoptosis by stabilizing RRBP1 in non-small cell lung cancer. Mol Oncol. 2022;16:1572–90. https://doi.org/10.1002/1878-0261.13112.
30. Ward PS, Thompson CB. Metabolic reprogramming: a cancer hallmark even warburg did not anticipate. Cancer Cell. 2012;21:297–308. https://doi.org/10.1016/j.ccr.2012.02.014.
31. Xiao Y, Jiang X, Yin K, Miao T, Lu H, Wang W, Ma L, Zhao Y, Liu C, Qiao Y, Zhang P. USP35 promotes cell proliferation and chemotherapeutic resistance through stabilizing FUCA1 in colorectal cancer. Oncogenesis. 2023;12:12. https://doi.org/10.1038/s41389-023-00458-2.
32. Zhang Q, Liu YJ, Li JP, Zeng SH, Shen H, Han M, Guo S, Liu SL, Zou X. USP35 is a Potential Immunosuppressive Factor in Skin Cutaneous Melanoma. J Inflamm Res. 2022;15:3065–82. https://doi.org/10.2147/jir.S362619.
33. Zhang J, Chen Y, Chen X, Zhang W, Zhao L, Weng L, Tian H, Wu Z, Tan X, Ge X, et al. Deubiquitinase USP35 restrains STING-mediated interferon signaling in ovarian cancer. Cell Death Differ. 2021;28:139–55. https://doi.org/10.1038/s41418-020-0588-y.
34. Motzer RJ, Penkov K, Haanen J, Rini B, Albiges L, Campbell MT, Venugopal B, Kollmannsberger C, Negrier S, Uemura M, et al. Avelumab plus Axitinib

versus Sunitinib for Advanced Renal-Cell Carcinoma. N Engl J Med. 2019;380:1103–15. https://doi.org/10.1056/NEJMoa1816047.
35. Rini BI, Plimack ER, Stus V, Gafanov R, Hawkins R, Nosov D, Pouliot F, Alekseev B, Soulières D, Melichar B, et al. Pembrolizumab plus Axitinib versus Sunitinib for Advanced Renal-Cell Carcinoma. N Engl J Med. 2019;380:1116–27. https://doi.org/10.1056/NEJMoa1816714.
36. Tang Z, Jiang W, Mao M, Zhao J, Chen J, Cheng N. Deubiquitinase USP35 modulates ferroptosis in lung cancer via targeting ferroportin. Clin Transl Med. 2021;11: e390. https://doi.org/10.1002/ctm2.390.
37. Cao J, Wu D, Wu G, Wang Y, Ren T, Wang Y, Lv Y, Sun W, Wang J, Qian C, et al. USP35, regulated by estrogen and AKT, promotes breast tumorigenesis by stabilizing and enhancing transcriptional activity of estrogen receptor α. Cell Death Dis. 2021;12:619. https://doi.org/10.1038/s41419-021-03904-4.
38. Yoriki K, Mori T, Kokabu T, Matsushima H, Umemura S, Tarumi Y, Kitawaki J. Estrogen-related receptor alpha induces epithelial-mesenchymal transition through cancer-stromal interactions in endometrial cancer. Sci Rep. 2019;9:6697. https://doi.org/10.1038/s41598-019-43261-z.
39. Bouris P, Skandalis SS, Piperigkou Z, Afratis N, Karamanou K, Aletras AJ, Moustakas A, Theocharis AD, Karamanos NK. Estrogen receptor alpha mediates epithelial to mesenchymal transition, expression of specific matrix effectors and functional properties of breast cancer cells. Matrix Biol. 2015;43:42–60. https://doi.org/10.1016/j.matbio.2015.02.008.
40. Gao H, Yin J, Ji C, Yu X, Xue J, Guan X, Zhang S, Liu X, Xing F. Targeting ubiquitin specific proteases (USPs) in cancer immunotherapy: from basic research to preclinical application. J Exp Clin Cancer Res. 2023;42:225. https://doi.org/10.1186/s13046-023-02805-y.
41. Chen, S., Liu, Y., and Zhou, H. (2021). Advances in the Development Ubiquitin-Specific Peptidase (USP) Inhibitors. Int J Mol Sci *22*. https://doi.org/10.3390/ijms22094546.
42. Futran, A., Lu, T., Amberg-Johnson, K., Yang, X., He, S., Bell, J., Boyce, S., Dahlgren, M., Dingley, K., Fang, L., et al. (2021). Abstract 1338: Discovery of novel, potent USP7 inhibitors that upregulate p53 leading to antiproliferative effects in cancer cells https://doi.org/10.1158/1538-7445.AM2021-1338.
43. Tian Z, D'Arcy P, Wang X, Ray A, Tai YT, Hu Y, Carrasco RD, Richardson P, Linder S, Chauhan D, Anderson KC. A novel small molecule inhibitor of deubiquitylating enzyme USP14 and UCHL5 induces apoptosis in multiple myeloma and overcomes bortezomib resistance. Blood. 2014;123:706–16. https://doi.org/10.1182/blood-2013-05-500033.

Publisher's Note